J Math Chem (2014) 52:430–440
DOI 10.1007/s10910-013-0270-4

ORIGINAL PAPER

Extended Poisson–Nernst–Planck modeling of membrane blockage via insoluble reaction products

Benjamin E. McNealy · Joshua L. Hertz

Received: 27 June 2013 / Accepted: 3 October 2013 / Published online: 13 October 2013

Abstract A generalized time-dependent mathematical model is developed for a diffusion–migration–reaction system incorporating a pore blockage effect due to generation of insoluble precipitates in a porous membrane. The system behavior is investigated via direct numerical solution of an extended, highly non-linear equation set based on the classical Poisson–Nernst–Planck equations for ion transport. In order to treat the buildup of solid reaction products in the membrane, this novel formulation incorporates both a reaction term and a space- and time-dependent diffusivity expression based on a simple precipitation model. The model is demonstrated for a generalized case and then extended to cover the well-known reaction of silver and chloride ions to form insoluble AgCl. Time-dependent concentration profiles of all ions in the membrane are obtained and the effects of precipitate buildup in the pore space are investigated. The role of counterions in the transient behavior of the system is also clarified.

Keywords Porous media · Ion transport · Precipitation

1 Introduction

The classical Nernst–Planck equations for ion transport in thin membranes have been much discussed in the literature, and numerical models have been developed for both steady-state and time-dependent ion dynamics [1]. More recently, the equations have also been extended to include reactions between species [2,3]. In the present work, a highly generalized diffusion–migration–reaction model considers the case where

B. E. McNealy (✉) · J. L. Hertz
Department of Mechanical Engineering, University of Delaware,
126 Spencer Laboratory, Newark, DE 19716, USA
e-mail: bmcnealy@udel.edu

reactions between ions form an insoluble product that physically interferes with species transport in the membrane. The system modeled here closely resembles plant transpiration experiments performed recently by Schreiber et al. [4] and, less directly, by Ranathunge et al. [5]. In those experiments, plant membranes were blocked by precipitation reactions when the membranes were suspended between two salt reservoirs. As will be seen, such a system exhibits unique characteristics, with the effect of the counterion of special interest. It is expected that highly similar models will have relevance to corrosion processes [6], biomineralization [7], and other areas.

Dilute electrochemical systems involving diffusion, migration, and chemical reactions [8] can be described by a form of the Nernst–Planck equation,

$$\frac{\partial c_i}{\partial t} + \nabla \bullet \left[-D_i \nabla c_i - z_i D_i c_i \frac{F}{RT} \nabla \varphi \right] - \sum_j r_{ij} = 0 \tag{1}$$

where c_i, D_i, and z_i are the concentration, diffusivity, and charge number, respectively, of the ith species, F is the Faraday constant, R is the molar gas constant, T is the absolute temperature, and φ is the electric potential. The final term in (1) is not commonly included in electrochemical systems; it describes the consumption or generation of species i due to chemical reactions with one or more other species j. The value and form of each source/sink term in the summation depends on the rate equation for the specific reaction being considered, and can be independent of reactant concentration (zero-order) or some higher-order function of the reactant concentration(s).

Since the electric potential φ in (1) is still unknown, an additional equation describing the electrostatic behavior of the system is required. A natural choice is Poisson's equation,

$$\nabla^2 \varphi = -\frac{F}{\varepsilon} \sum_i z_i c_i \tag{2}$$

where ε is the absolute permittivity of the medium. Thus the complete set of governing equations is given by (1) and (2).

In a porous membrane, an effective diffusivity [9] can be expressed as

$$D_{eff} = D_{aq} \varepsilon_t \delta / \tau_f \tag{3}$$

where D_{aq} is the diffusivity in water and the dimensionless parameters ε_t, δ, and τ_f are the porosity, constrictivity, and tortuosity of the membrane, respectively. Equation (3) assumes that diffusion occurs only in the pore space and not in the solid phase of the membrane. The most important of these in the present case is the porosity, which is defined as the volume fraction of pore space in the membrane ($0 \leq \varepsilon_t \leq 1$). Typical porosities for porous membranes range from 0.3 to 0.7 [10]. In the system being considered here, the diffusivity is allowed to vary as a function of space and time, since pores can become locally constricted by the precipitation reaction. The tortuosity ($\tau_f \geq 1$) of a typical porous membrane is in the range 1.5–2.5 [10], while

constrictivity ($0 \leq \delta \leq 1$) is approximately 1 when the membrane pores are large compared to the diffusing species [9].

2 Methods

As this system was expected to be highly non-linear, numerical modeling was used to explore its behavior. Non-linearity arises from diffusivity values that not only vary in space and time, but also depend on the time-integrated local precipitation rate. The precipitation reaction in turn requires the diffusion of additional reactants to persist. A one-dimensional, time-dependent numerical model was developed using COMSOL Multiphysics (version 4.3a, COMSOL AB). To demonstrate the behavior of a diffusion–migration–reaction system including insoluble reaction products, the model was initially implemented for a generalized system involving a reaction of the form $A^{+}_{(aq)} + B^{-}_{(aq)} \longrightarrow AB_{(s)}$. The system consists of a hydrated porous membrane of thickness L positioned between two reservoirs containing 0.1 mol/L solutions of AM and BN, respectively, where M^{-} and N^{+} are unreactive counterions. All four species can diffuse and migrate within the water-filled pores of the membrane. While equilibrium concentrations of H^{+} and OH^{-} ions are also present in the pore fluid, these species were neglected since their concentrations are negligible compared to those of the other ions. The complete set of governing equations in the model therefore consists of the single equation (2) and a set of five equations of the form (1), one for each of the species A^{+}, B^{-}, M^{-}, N^{+}, and AB.

The A^{+} and B^{-} ions react to form the insoluble product AB, which precipitates out of solution to create a solid obstruction in the membrane pores. Assuming second-order kinetics, the rate equation for AB formation is given by

$$r_{AB} = k_{AB}\left(c_A c_B - K_{sp,AB}\right) \tag{4}$$

where k_{AB} is the reaction rate coefficient and $K_{sp,AB}$ is the solubility product. For computational simplicity it was assumed that AB is ideally insoluble, i.e. $K_{sp,AB} = 0$. The accumulation of solid reaction products causes a local reduction in porosity and, therefore, in the effective diffusivities of all mobile species in the membrane. Neglecting nucleation effects, which are unlikely to be a concern given that the system is heterogeneous, the relative amount of pore volume filled with precipitate is simply the product of its concentration and molar volume. The precipitates are assumed to be equiaxed on average such that the amount of pore cross-sectional area being displaced is equal to the portion of the volume filled with precipitate, and the effective diffusivities of all species traveling through the membrane are in proportion to the cross-sectional area of the pore phase. Expanding (3) to incorporate these considerations, a new model for effective diffusivity was developed:

$$D_{eff}(x,t) = \left(\delta/\tau_f\right)\left(\varepsilon_{t0} - V_{AB}c_{AB}(x,t)\right) D_{aq} \tag{5}$$

where ε_{t0} is a globally defined initial porosity and $c_{AB}(x,t)$ and V_{AB} are the concentration and molar volume, respectively, of AB precipitate. As the precipitation reaction

(4) proceeds, the local value of c_{AB} increases, causing a corresponding decrease in the local effective diffusivity.

Perhaps contrary to initial appearances, Eq. (5) is well-posed and does not allow for negative effective diffusivities when placed in the broader context of the system being modeled. Equations (1) and (4) couple c_{AB} to the local effective diffusivities of the reactants such that as the precipitation reaction proceeds, the diffusion of further reactants is slowed. A negative feedback cycle thus exists between the precipitate concentration and the precipitate reaction rate. Eventually, given well-posed initial and boundary conditions, the reaction extinguishes itself before negative diffusivity values can be reached. Nevertheless, when using computationally feasible time and space discretizations, the extremely large concentration gradients created near the reaction front in this highly nonlinear system were found to occasionally yield erroneous negative values of local concentration and diffusivity, which resulted in non-convergence of the model. While it is expected that convergence could be obtained by refining the discretization, this proved to be impractical given the computing power available. Therefore, a minimum threshold porosity value ε_{min} was implemented. For ε_{min} sufficiently close to zero, real system behavior remains well modeled. Numerical stability of the model was obtained here for a value of $\varepsilon_{min} = 1 \times 10^{-6}$.

Rather than offering a detailed description of the behavior in a single pore as in, for example, Ref. [11], the one-dimensional continuum-level treatment just described seeks to quantify the average behavior across the entire cross-sectional space of a porous medium. Specifically, (5) necessarily implies the physical intuition that blockage in one pore does not prevent diffusion in a neighboring pore, and can thus provide a better description of complete membrane behavior than single pore models. In the present case, the initial porosity of the membrane was taken as 0.5 (indicating a pore content of 50 % by volume), which is typical of real membranes [10].

Tortuosity and constrictivity effects were neglected by setting δ and τ_f to unity, as these parameters were not of interest to the present study and would only serve to uniformly decrease the effective diffusivity values. For simplicity, the initial (unconstricted) diffusivities of all four mobile ion species were taken as $1.5 \times 10^{-9}\mathrm{m}^2/\mathrm{s}$, while the precipitate species was assumed to be completely immobile. The precipitate and the solid membrane scaffold were assumed to be impermeable to ion transport.

Boundary conditions for the Nernst–Planck equations were of the form

$$\begin{aligned} c_i(0,t) &= c_{0,i} \\ c_i(L,t) &= c_{L,i} \end{aligned} \tag{6}$$

where the concentrations of the ith species in the left and right bathing solutions are given by $c_{0,i}$ and $c_{L,i}$, respectively. In the case of a 0.1 mol/L AM solution at the left boundary and a 0.1 mol/L BN solution at the right boundary, the reservoir concentrations are $c_{0,A} = c_{0,M} = c_{L,B} = c_{L,N} = 100\ \mathrm{mol/m}^3$ and $c_{0,B} = c_{0,N} = c_{L,A} = c_{L,M} = 0$. To improve model stability, the reservoir concentrations were ramped from zero to the steady-state values given above over the first 0.5 s of the simulation using a smoothed step function. The reservoirs were assumed to be large enough that any change in the bathing solution concentrations from the initial values is negligible.

In the initial state, the membrane contained zero concentrations of all species. Electrical boundary conditions were specified with the left boundary electrically grounded and a zero-charge condition (i.e. $\vec{n}\bullet\nabla\varphi = 0$) at $x = L$ in order to allow the potential across the membrane to float freely.

The effect of varying the ion mobilities in the system was examined by replacing the generalized A^+ and B^- species with silver and chloride ions, respectively, which are subject to the well-known precipitation reaction $Ag^+_{(aq)} + Cl^-_{(aq)} \longrightarrow AgCl_{(s)}$. In recent experimental work, Schreiber et al. [4] formed AgCl precipitates as a means to block aqueous pores in an isolated plant cuticle by suspending it between reservoirs of 0.01 M NaCl and 0.01 M $AgNO_3$. The rate equation for AgCl formation is

$$r_{AgCl} = -k\left(c_{Ag}^{1/2}c_{Cl}^{1/2} - c_0\right)^2 \tag{7}$$

where k is the reaction rate coefficient and c_0 is the solubility of AgCl [12]. As this solubility is at least three orders of magnitude smaller than the species concentrations [13] the c_0 term in (7) is neglected here for computational simplicity. With this simplification the rate equation for AgCl formation is of the same form as (4). The value of k was taken as $4.2\ \mathrm{m}^3/(\mathrm{mol\ s})$ as given in [12]. In addition, the generalized counterion species were replaced with various combinations of actual soluble species (lithium, sodium, and potassium cations, and nitrate and acetate anions). The tendency toward local electroneutrality implied by Eq. (2) suggests that the diffusion of the reacting ions may be suppressed by a slower diffusing counterion. All diffusion coefficients used were obtained from tabulated values in water [13]. The parameter values used in the model are summarized in Table 1.

3 Results and discussion

Time-dependent concentration profiles for the generic reactive ions (A^+ and B^-) are shown in Fig. 1, and the corresponding profiles for the generic unreactive ions (M^- and N^+) are shown in Fig. 2. The time-dependent behavior of the system consists of an initial transient period followed by a metastable period where concentrations change slowly over time, a second transient period, and a final steady state. Beginning at $t = 0$, ions begin to enter the porous membrane and a reaction front is established at the midpoint of the membrane as the A^+ and B^- ions begin to meet and annihilate each other. An initial near-steady state is established after approximately 5 s, which is on the order of the characteristic diffusion time L^2/D. In this state, the concentration profiles of the unreactive ions are nearly linear, as would be expected for a simple diffusion between two reservoirs of constant concentration. In contrast, the concentrations of the reactive ions are sub-linear due to the depletion of ions at the reaction front. Without the precipitation of the reaction product, this would remain the final state of the system.

Between approximately $t = 5$ and $t = 135$ s, the ion concentration profiles in the membrane change gradually as precipitate builds up in the membrane pores. The effective membrane porosity due to this reaction product buildup is shown in Fig. 3. As the effective porosity within the reaction zone decreases, the ion concentration gradients around this region gradually increase. At approximately $t = 140$ s, the

Table 1 Parameters used in the model

Symbol	Meaning	Value	References
D_{aq}	Unconstricted diffusivity		
	A^+, B^-, M^-, N^+	1.5×10^{-9} m^2/s	–
	Ag^+	1.65×10^{-9} m^2/s	[13]
	Cl^-	2.03×10^{-9} m^2/s	[13]
	CH_3COO^-	1.09×10^{-9} m^2/s	[13]
	K^+	1.96×10^{-9} m^2/s	[13]
	Li^+	1.03×10^{-9} m^2/s	[13]
	Na^+	1.33×10^{-9} m^2/s	[13]
	NO_3^-	1.90×10^{-9} m^2/s	[13]
L	Membrane thickness	0.1 mm	–
V_{AB}	Precipitate molar volume	2.58×10^{-5} m^3/mol	[13]
k_{AB}	Reaction rate constant	4.2 m^3/(mol s)	[12]
ε	Absolute permittivity of water	7.08×10^{-10} F/m	[13]
δ	Membrane constrictivity	1	–
ε_{t0}	Initial membrane porosity	0.5	–
τ_f	Membrane tortuosity	1	–

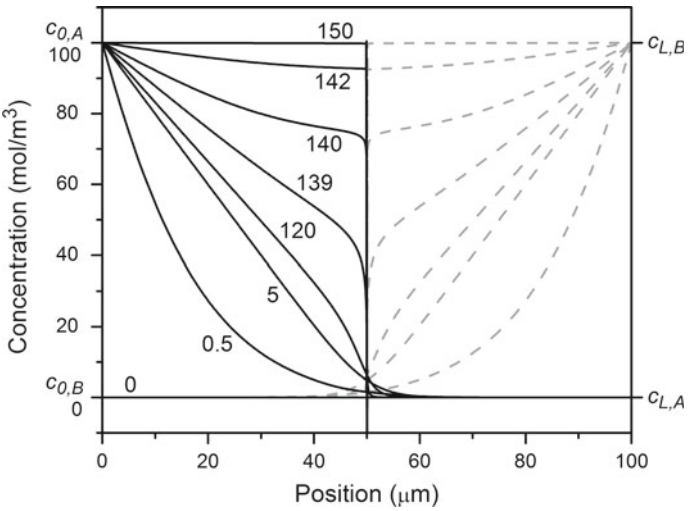

Fig. 1 Concentration profiles for reactive ions A^+ (*solid lines*) and B^- (*dashed lines*) at several instants of time indicated in seconds after initiating ion flux at $t = 0$. Reservoir concentrations are indicated at the boundaries

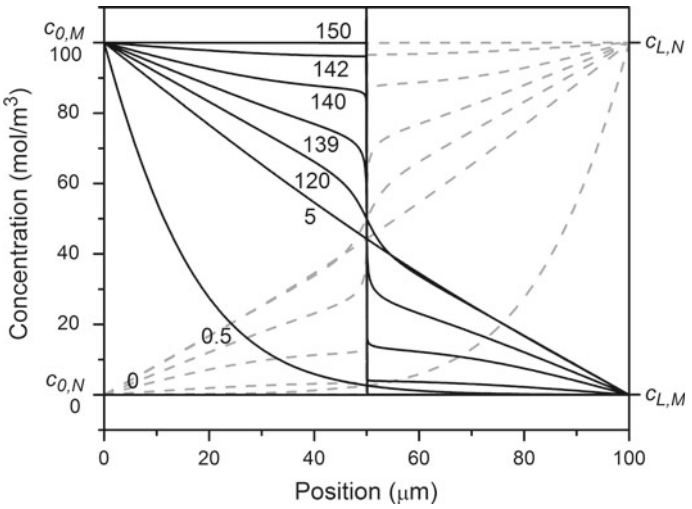

Fig. 2 Concentration profiles for unreactive counter-ions M^- (*solid line*) and N^+ (*dashed line*) at several instants of time indicated in seconds after initiating ion flux at $t = 0$. Reservoir concentrations are indicated at the boundaries

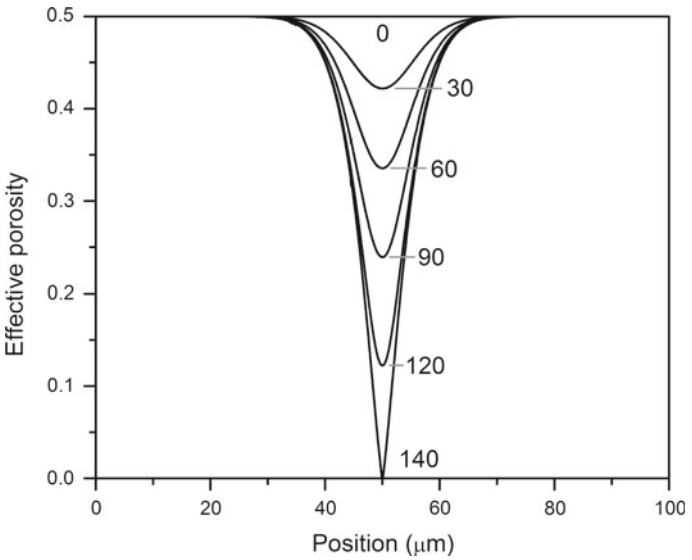

Fig. 3 Local effective porosity in the membrane at several instants of time indicated in seconds after initiating ion flux at $t = 0$

effective porosity at the center of the reaction zone reaches the near-zero minimum value allowed by the model and the local diffusivities of all ions become negligible. At this point, fresh A^+ and B^- reactants are prevented from diffusing to the reaction front in appreciable quantities, and their concentrations quickly approach a constant value on either side of the blockage as ions diffuse inward from the boundaries. The

concentrations of N^+ ions on the left side of the obstruction and M^- ions on the right side approach zero as the counterions diffuse back out of the membrane into the reservoirs, as dictated by the boundary conditions. In the final steady state, seen at $t = 150$ s in Figs. 1 and 2, the concentration profiles of all ions resemble step functions with uniform concentrations nearly equal to the reservoir concentrations on either side of the blockage. The time required to establish the final steady state once the membrane is blocked is approximately 5 s, which again is on the order of the characteristic diffusion time of the ions through the membrane.

The inward fluxes of all four species at the left boundary (i.e. $x = 0$) are shown in Fig. 4a. As the membrane is exposed to the AM bathing solution at $x = 0$, this boundary experiences an inward flux of A^+ and M^- and an outward flux of N^+, while the flux of B^- is very close to zero since no appreciable quantity of B^- ions reaches the left side of the reaction zone. (The flux behavior at $x = L$ is identical but with the roles of the AM and BN solutions reversed.) The fluxes of A^+ and M^- are initially equal due to the constraint imposed by Poisson's equation, but once N^+ counterions are locally available to maintain charge balance the flux of M^- at the boundary decreases to approximately half that of A^+. The reason for this difference in flux is that the driving force for inward flux of A^+ is a gradient in concentration reaching zero at the reaction front halfway across the membrane while the driving force for inward flux of M^- is a gradient in concentration reaching zero at the interface with the BN solution all of the way across the membrane. During the metastable period (approximately $10\,\text{s} < t < 135\,\text{s}$), the inward fluxes of A^+ and B^- are balanced by their mutual annihilation at the reaction front, while the fluxes of M^- and N^+ into the domain are balanced by equal outward fluxes at the opposite boundaries. The change in flux

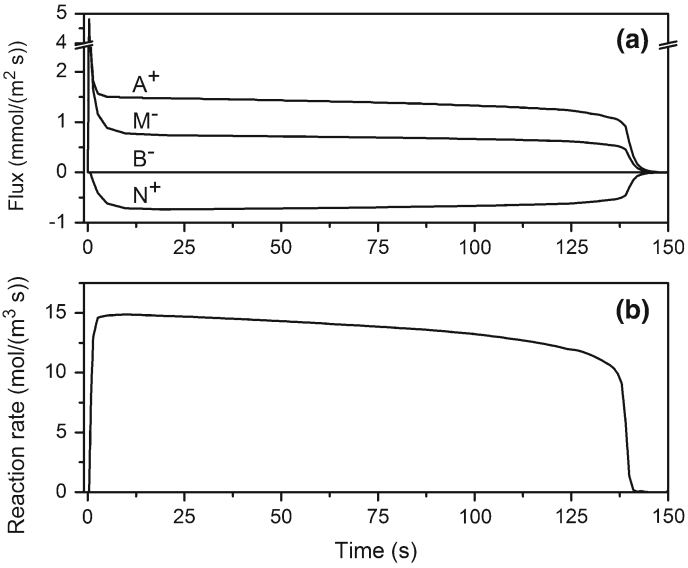

Fig. 4 **a** Inward flux of each ionic species in mmol/(m^2 s) at $x = 0$ as a function of time (note axis break). **b** Net (integrated) reaction rate in mol/(m^3 s) as a function of time

with time is initially linear, but becomes more rapid as the increasing concentration gradients cause the reaction zone to become more spatially concentrated. After the effective porosity becomes negligible at $t = 140$ s the fluxes quickly drop off to near zero as only minute quantities of ions are able to penetrate the reaction zone, and steady state is obtained.

The spatially integrated reaction rate (i.e., total rate of AB production throughout the membrane) as a function of time is shown in Fig. 4b. This plot shows a similar trend to Fig. 4a, with a gradual decrease in reaction rate over the metastable period followed by a rapid dropoff at approximately $t = 140$ s. Although the net reaction rate shown in the figure decreases over the course of the near-steady period, the *maximum* local reaction rate (not shown) increases over the same period as the reaction zone becomes narrower and the reactant concentrations increase.

The above modeling provides a good description of "ideal" diffusion, migration, and precipitation processes in a porous membrane. However, the generalized system is somewhat unrealistic in that the mobilities of all ionic species are equal. In order to put the above results on a more realistic footing, the model was modified by replacing the generalized A^+ and B^- ions with silver and chloride ions, respectively, which react according to $Ag^+_{(aq)} + Cl^-_{(aq)} \longrightarrow AgCl_{(s)}$. To investigate the role of the counterion species, six different cases were modeled (one for each possible combination of Li^+, Na^+, and K^+ cations and NO_3^- and CH_3COO^- anions). While these substitutions have a negligible effect over large timescales, the initial transient behavior is quite different from the generalized case.

Without an applied voltage across the membrane, the effect of ion charge is subtle but tied to presence of counterions. In the initial state of the modeled system, the aqueous phase is free of charge, and thus the initial diffusion of the ions from either side is limited by the diffusivity of the slower ion in each bathing solution. Specifically, the initial diffusion of the faster species is held back by the development of a counteracting electric field arising from the local charge imbalance. The initial reaction zone location where the Ag^+ and Cl^- begin to form precipitate thus depends on the identity of the counterions in the bathing solutions. Figure 5 shows the position of the reaction zone as a function of time for all six different combinations of counterions. Results are shown only for $t > 3$ s as the position of the reaction front could not be reliably determined at earlier timesteps.

The theoretical initial location of the reaction zone, l_0, is determined by the ratio of the diffusion lengths of the slower ion in each bath. Since the diffusion length is proportional to the square root of diffusivity, l_0 is expected to be proportional to the dimensionless ratio

$$R = \frac{\sqrt{D_1}}{\sqrt{D_1} + \sqrt{D_2}} \tag{8}$$

where D_1 and D_2 are the diffusivities of the slower ion in the left and right bath, respectively. The inset in the figure plots the position of the reaction zone at $t = 3$ s as a function of this ratio, showing the expected linear dependence. Interestingly, while the initial position of the reaction zone depends on the counterion, the final location of the precipitate remains largely the same in each of the six cases. This occurs because

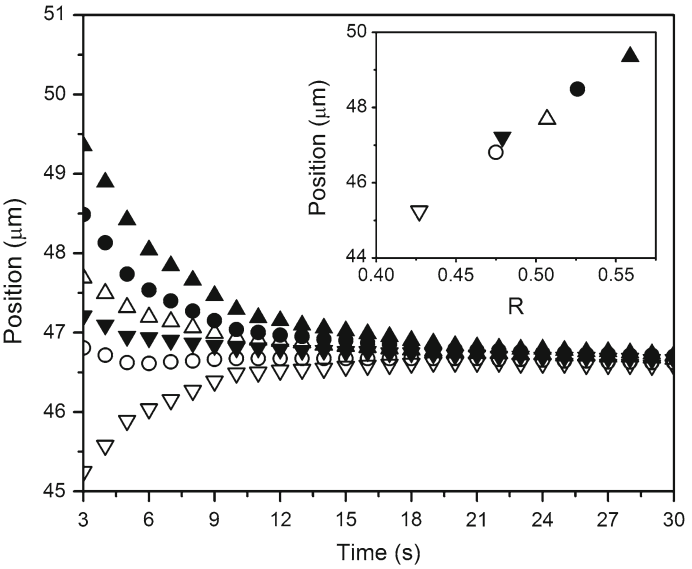

Fig. 5 Position of the reaction front versus time for several different counterion species. Positive counterions (N^+) are Li^+ (*upward triangles*), Na^+ (*circles*), and K^+ (*downward triangles*); negative counterions (M^-) are $NaNO_3^-$ (*solid symbols*) and CH_3COO^- (*open symbols*). *Inset*: Initial position ($t = 3$ s) of the reaction front versus the dimensionless quantity R given by (8)

once the initial reaction zone is established, the counterions have filled the membrane and further diffusion of the reacting species ceases to be determined by the diffusivity of the counterions. Since the reaction has only started to proceed at this point, it would seem impossible to specify the location of the precipitate using this effect. The precipitate blockage in a porous membrane will be located at a position determined by the relative diffusion lengths of the *reacting* ions, which is around $0.46 \cdot L$ for AgCl.

4 Conclusions

The behavior of a diffusion–migration–reaction system with insoluble reaction products was investigated via numerical modeling. The system was modeled using the Poisson–Nernst–Planck equations along with a time- and space-dependent diffusivity expression to account for physical obstruction caused by the buildup of solid products of reaction between diffusing ions. The specific systems modeled consisted of reservoirs containing generalized aqueous solutions "AM" and "BN" positioned on either side of a hydrated porous membrane followed by the specific case used in previously reported experimentation using $AgNO_3$ and NaCl solutions. Various combinations of counterions were also investigated. An initial near-steady state is quickly established with a reaction zone at the center of the domain. As precipitate builds up in the reaction zone, the effective local ion diffusivities approach zero and concentration gradients become large. The system reaches a final steady state where all species exhibit a step concentration change at the reaction zone. Transients establishing the first metastable

state and then the final steady state occur over timescales related to the diffusion of ions through the membrane. The effect of varying the ion diffusivities is small, changing only the initial site of the precipitation reaction. It is believed that generalized PNP modeling of this sort can be useful in the future to quantitatively understand other situations where ion reactions and/or phase transformations affect ion motion.

References

1. H. Cohen, J.W. Cooley, Biophys. J. **5**, 145 (1965)
2. D. Šnita, M. Marek, Phys. D **75**, 521 (1994)
3. J.H. Merkin, P.L. Simon, Z. Noszticzius, J. Math. Chem. **28**, 43 (2000)
4. L. Schreiber, S. Elshatshat, K. Koch, J. Lin, J. Santrucek, Planta **223**, 283 (2006)
5. K. Ranathunge, E. Steudle, R. Lafitte, Plant Cell Environ. **28**, 121 (2005)
6. S.M. Sharland, Corros. Sci. **33**, 183 (1992)
7. H. Yin, B. Ji, P.S. Dobson, K. Mosbahi, A. Glidle, N. Gadegaard, A. Freer, J.M. Cooper, M. Cusack, Anal. Chem. **81**, 473 (2009)
8. B.E. McNealy, J.L. Hertz, Int. J. Hydrogen Energy **38**, 5357 (2013)
9. P. Grathwohl, *Diffusion in Natural Porous Media* (Kluwer Academic Publishers, Norwell, 1998)
10. R. Baker, *Membrane Technology and Applications* (Wiley, Hoboken, 2012)
11. M.-T. Wolfram, M. Burger, Z.S. Siwy, J. Phys. Condens. Matter **22**, 454101 (2010)
12. C.W. Davies, G.H. Nancollas, Trans. Faraday Soc. **51**, 818 (1955)
13. D.R. Lide (ed.), *CRC Handbook of Chemistry and Physics*, 74th edn. (CRC Press, Boca Raton, 1993)